Enhancing Performance of Li4Ti5O12 with Addition of Activated Carbon from Recycled PET Waste as Anode Battery Additives

Priyono, Bambang
Department of Metallurgical and Materials Engineering, Universitas Indonesia

Rifky, Baron
Department of Metallurgical and Materials Engineering, Universitas Indonesia

Zahara, Frida
Department of Metallurgical and Materials Engineering, Universitas Indonesia

Subhan, Ahmad
Research Center for Physics - LIPI, PUSPIPTEK

https://doi.org/10.5109/4794188

出版情報：Evergreen. 9 (2), pp.563-570, 2022-06. 九州大学グリーンテクノロジー研究教育センター
バージョン：

Enhancing Performance of Li4Ti5O12 with Addition of Activated Carbon from Recycled PET Waste as Anode Battery Additives

Bambang Priyono[1,*], Baron Rifky[1], Frida Zahara[1], Ahmad Subhan[2]
[1]Department of Metallurgical and Materials Engineering, Universitas Indonesia, Depok, 16424, Indonesia
[2]Research Center for Physics – LIPI, PUSPIPTEK, Tangerang, Banten, 15310, Indonesia

*bpriyono@metal.ui.ac.id

(Received February 11, 2022; Revised June 20, 2022; accepted June 20, 2022).

Abstract: The rapid development of the industry makes the amount of plastic waste increase. The difficulty of plastic waste to be degraded makes its handling important to avoid environmental pollution. This research converts plastic waste into activated carbon with to increase the economic value by apply the activated carbon as an anode battery additive. Li4Ti5O12 has advantages as a lithium ion battery such as a good level of safety and thermal stability but poor conductivity. The recycled carbon is activated using NaOH to obtain a porous structure that can increase the conductivity of the LTO/C composite. The activated carbon itself has conductivity of 9,65.10-5 S/m. The effect of activated carbon to the overall battery performance was being studied in this research. This study synthesized LTO/C using the ball-milling method with variations of 90 minutes, 120 minutes, and 150 minutes milling to determine the optimum composite synthesis time for the battery. The EIS test showed that the addition of activated carbon was able to increase the LTO conductivity. Based on the results of EIS, CV and CD the optimal ball mill time is 90 minutes to produce a battery with the best performance and has the lowest resistance and a specific capacity of 149,8 Ω.

Keywords: battery anode, graphene, plastic waste, LTO, activated carbon, mixing time

1. Introduction

The rapid development of science and technology and industrial activities make the intensity of the use of plastic in product manufacturing and the amount of plastic waste gradually increase. Plastic waste can pollute the environment due to the nature of plastic's resistance to degradation which makes it very difficult to be assimilated by nature[1)]. Indonesia itself produces around 14% of plastic waste every day, which is equivalent to 85,000 tons per year and is considered not to be managed properly[2)]. As a result, as much as 3.2 million tons of waste produced by Indonesia is not managed and dumped into the sea, causing damage to the marine environment[3)]. Plastic waste is generally handled in three ways: discarded, incinerated, and recycled. It is estimated that until 2050 the amount of plastic waste that is recycled is still much lower than the amount that is discarded[1)]. To be able to improve its implementation, the recycling method must be able to offer more added value and incentives than other alternatives, one way is by producing recycled products that have high economic value.

Carbon is an ideal material for energy storage as an electrode material in lithium ion batteries. Lithium ion batteries are often used in portable electronic devices and electric vehicles (EVs) due to their high capacity and long cycle life[4,5)]. A lot of research related to electric vehicles is now being carried out to support market growth of around 60 percent per year[6)]. Graphite is a form of carbon that is commonly used in lithium ion batteries but has drawbacks such as limited lithium diffusion kinetics[7)]. LTO (Li4Ti5O12) outperformed graphite as an anode material with a voltage of 1.55 V vs. Li/Li+ which makes it does not form a solid electrolyte interphase (SEI) layer, does not change in volume, and has a very good level of safety and thermal stability[8)]. The disadvantage of LTO is that its low conductivity limits the charge/discharge rate of the battery.

Many research on processing waste into carbon electrodes have been carried out, especially on biomass waste such as rice straw, rice husks, coffee husks, plant stems, green tea, and sisal[9)]. In this case, the precursor and the method used will affect the structure, characteristics and electrochemical performance of the carbon product. The synthesis process and characteristics of LTO/C composites and the effect of adding activated carbon from PET plastic waste to the LTO anode were investigated in this experiment.

2. Materials and Method

2.1 Materials

Materials that will be used in this research are Li4Ti5O12 from Sigma Aldrich, polyethylene terephthalate collected from municipal waste, hydrochloric acid from Merck, and natrium hydroxide from Merck.

2.2 Synthesis of Carbon

This study utilizes PET plastic waste as a precursor for the synthesis of carbon to be activated carbon material with pyrolysis method. The first stage is the preparation of plastic waste by collecting a number of PET bottle waste which is then shredded into small pieces of uniform size. The PET bottle waste most likely still has a lot of dirt and oil attached, so it is cleaned using soap and then dried. Then the clean plastic waste is weighed and mixed with bentonite with a mixing ratio of 8:2. Bentonite serves as a catalyst in the carbonization process. The mixture of plastic flakes and bentonite was carbonized using a tube furnace in an inert nitrogen atmosphere with a heating rate of 5˚C per minute to reach a temperature of 400˚C and held for 2 hours. The result is amorphous carbon ground using a ball mill to form a fine powder of carbon.

2.3 Carbon Activation Process

The next step is carbon activation, amorphous carbon powder is mixed with NaOH in a ratio of 1:3 using a magnetic stirrer for 2 hours. The mixture was heated for 4 hours at a temperature of 130˚C and then sintered in a nitrogen gas stream at a temperature of 700˚C for 1.5 hours with a heating rate of 20˚C. The sintered product was washed with warm distilled water and 0.1 M HCl solution to neutralize the solution. Then the result is heated at 110˚C for 24 hours to produce activated carbon powder. After the activation process is complete, the activated carbon has formed a pore structure. according to the literature the mixing ratio for the optimum activation results when using NaOH reagent is 1:3[10]. Therefore, activated carbon samples with this ratio will be used in this study to make batteries in order to study the effect of the synthesis time of anode active materials on battery performance.

2.4 Synthesis of $Li_4Ti_5O_{12}$ – Activated Carbon

Synthesized activated carbon powder with an activation ratio of 1:3 in the amount of 3 wt% was mixed with commercial LTO by mechanochemical method using a high energy ball mill. This process takes place at a speed of 1560 rpm (26 Hz) with time variations of 60, 120 and 180 minutes, where every 30 minutes a resting time is carried out for 10 minutes. In the mixing process, ±10 ml of ethanol was added to prevent agglomeration. The resulting mixture was dried using a hot plate and after that the mixing product was obtained, namely the LTO/C composite.

2.5 Battery Fabrication Process

Composites consisting of a mixture of LTO and activated carbon with an activation ratio of 1:3 were assembled into a coin cell so that their electrochemical abilities could be measured. In this stage, polyvinylidene fluoride (PVDF) binder, acetylene black (AB) conducting agent, and LTO/carbon active material were mixed in a ratio of 1:1:8 into 5.5 ml of dimethylacetamide (DMAC) at 65°C using magnetic stirrer to obtain a slurry with the desired viscosity. The slurry is then coated on a Cu sheet to form an anode which after drying will be cut into a circle and assembled into a CR2032 type coin cell. The slurry making process, coating and coin cell assembly is carried out at the LIPI Physics Laboratory, Serpong.

Table 1. composition and stirring time of each sample for slurry making process

Materials	LTO/C (g)	PVDF (g)	AB (g)	Stirring Time (minutes)
LTO/C 3% - 90 minutes	0,5019	0,0645	0,0628	128
LTO/C 3% - 120 minutes	0,5017	0,0648	0,0625	102
LTO/C 3% - 150 minutes	0,5021	0,0644	0,0622	121

2.6 Characterization and Performance Tests

To determine the characteristics of activated carbon, Scanning Electron Microscopy (SEM), Brunauer-Emmett-Teller (BET) and X-Ray Diffraction (XRD) tests were carried out. XRD and SEM-EDS (energy dispersive spectroscopy) characterization were performed on LTO/C samples. The BET test aims to determine the surface area and characteristics of the pores formed on activated carbon. XRD serves to detect the presence of any elements and phases contained in the sample. SEM aims to analyze the shape, structure, and topography of the sample results.

battery anodes performance is tested through Charge-Discharge (CD), Cyclic Voltammetry (CV), and Electrochemical Impedance Spectroscopy (EIS) tests. CV shows the potential values, anodic and cathodic peaks, and reversibility of the battery sample. CD to determine charge-discharge capability at various current rate conditions. Through the EIS test the impedance value of the battery can be determined and used to measure the conductivity of the sample.

3. Results and Discussion

3.1 Activated Carbon's Surface Characteristic

After activation with NaOH, the surface area of activated carbon will increase by the formation of pores. Figure 1a depicted the active carbon isotherm curve of N2 adsorption is increasing until one point, this curve is the characteristic of Isotherm Type 1 according to IUPAC which indicates formation of micropores[11]. Figure 1b

depicted carbon active pores distribution that ranges from 0,3 – 0,8 nm and included to micropores (0,1 – 1 nm) resulting the specific surface area of 459,352 m2/g. This surface area is still relatively low comparing to KOH activated carbon and the pores formed micropores instead of mesopores which sufficient for lithium intercalation. This limitation is because the natrium can only intercalate in on the low structural order material up to lower temperature of 450 ^{0}C, heating above this temperature will not resulting many changes after contact with natrium gas because no intercalation occur. Meanwhile, in this research the carbon was activated on 700 ^{0}C which result on redundancy[12]. On low ordered carbon structure, sodium is only able to be intercalated in highly defective materials especially on the interstition[13]. However, the impurities from bentonite resulting substitutive deformation which make NaOH could not intercalate well.

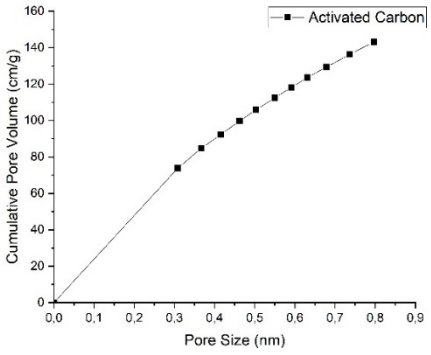

(a)

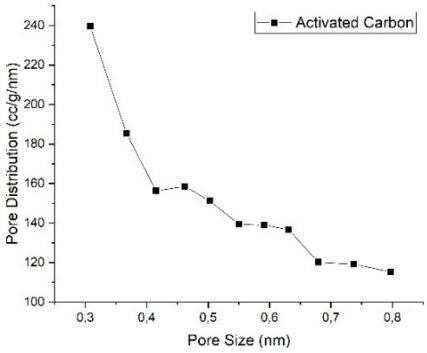

(b)

Fig. 1: (a) carbon active cumulative pore volume (b) activated carbon pore distribution.

3.2 Phase Analysis of Activated Carbon and LTO/C

The diffraction peak is identified using Crystallography Open Database (COD). The activated carbon shows the characteristic of activated carbon diffraction that has wide peak on 2θ = 430 and has no sharp peak on 26,370 that indicates the carbon formed is not graphite. XRD results of activated carbon in figure 2a shows wide and fuzzy diffraction peak that depicted indicating a turbostratic structure, which implies that the composition of graphitic-like microcrystallites that are randomly oriented and well distributed throughout the samples[14] and no sharp peak that indicate the full formation of amorphous or not oriented structure[15]. Figure 2a depicted wide and fuzzy peak as the characteristic of activated carbon and sharp peaks that detected are impurities phases which are Fe12 with 2θ = 22 (COD 96-431-0031), CaMg2 with 2θ = 360 (COD 96-900-6621), Ca4Mg3Al5 with 2θ = 340 (COD 96-431-3241), and Fe10Si with 2θ = 460 (COD 96-900-6621). The impurities phases came from the bentonite catalyst which uncleaned or untreated.

Figure 2b shows the diffraction of LTO/C samples. The main phase that identified according to pattern and peaks is Li10.67Ti13.33O32 (COD 96-100-1099). LTO/C 3% - 90 minutes has 3 highest peaks with 2θ position of 18,60, 43,4 0, dan 35,80. LTO/C 3% - 120 minutes has 3 highest peaks with 2θ position of 18,70, 43,50, dan 35,90. Lastly, LTO/C 3% - 90 minutes has 3 highest peaks with 2θ position of 18,60, 43,4 0, dan 35,80. LTO/C 3% - 150 minutes has 3 highest peaks with 2θ position of 18,50, 43,40, dan 35,70. The three samples shows similar peak position that indicate the phases formed are the same.

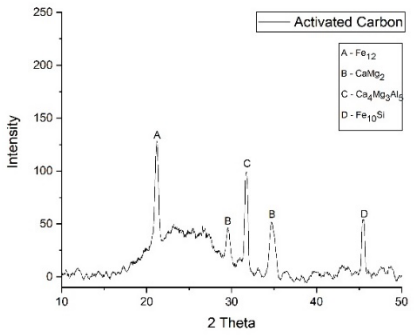

(a)

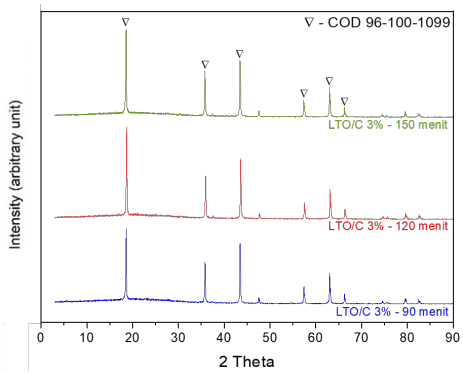

(b)

Fig. 2: XRD results of (a) activated carbon (b) LTO/C composites.

3.3 Morphology of Activated Carbon and LTO/C

The natrium in activation step works by intercalate on

the carbon particle surface resulting the reduction of carbon size. The carbon active has relatively smooth and homogenous particle. From the SEM image and particle size distribution of activated carbon in figure 2a and 2b, it clarifies that the resulting active carbon size ranging from 30 – 100 µm with pore size of 0,3 – 0,8 nm according to BET characterization.

The SEM image of LTO/C composites in figure 2b-d show the LTO particle clearly but the activated carbon is unseen which assumed that the activated carbon particle size has already reduced and well mixed by the employment of ball milling. LTO/C 3% - 90 minutes sample has the highest average particle size of 0,524 µm, following by the LTO/C 3% - 120 with the size of 0,471 µm and LTO/C 3% - 150 with the size of 0,366 µm as the smoothest particle size. According to the histogram in the figure 2f-h, LTO/C 3% - 120 minutes has the poorest distribution which is broader than the other two sample. Meanwhile, LTO/C 3% - 90 minutes has more uniform particle size which depicted by the narrow distribution. The particle size and distribution have influence to the battery electrode perform because the uniform size distribution and less agglomeration particle will be resulting better capacity retention[16].

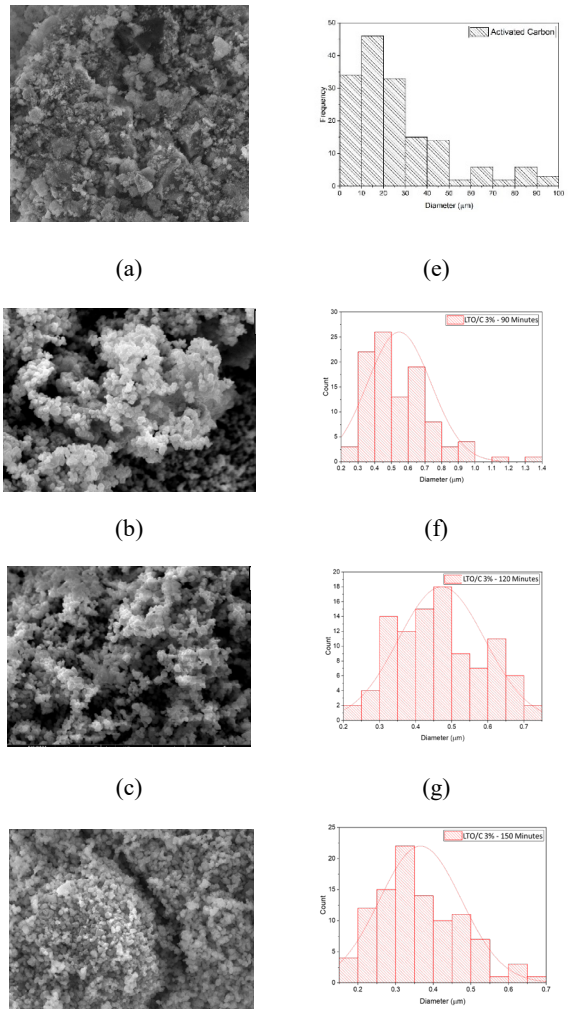

(a) (e)

(b) (f)

(c) (g)

(d) (h)

Fig. 3: SEM image of (a) activated carbon (b) LTO/C 3% - 90 minutes (c) LTO/C 3% - 120 minutes (d) LTO/C 3% - 150 minutes, particle size distribution of (e) activated carbon (f) LTO/C 3% - 90 minutes (g) LTO/C 3% - 120 minutes (h) LTO/C 3% - 150 minutes

Figure 4 shows the EDS characterization results in spectrums of each sample that inform the elements contained in that area. Table 1 presents the total of each element in the spectrums. The element contained in each spectrum in the same sample have significantly different amount which indicate the mixing had not result the homogenous phase. The Si indicated as the impurities from the bentonite catalyst from the pyrolysis.

Table 2. EDS characterization results of LTO/C

Sample	*Spectrum*	Element (wt%)			
		Ti	O	C	Si
LTO/C 3% - 90 minutes	2	41	55,7	3,3	-
LTO/C 3% - 120 minutes	5	57,1	42,9	-	-
	6	100	-	-	-
LTO/C 3% - 150 minutes	7	39,2	55,1	5,3	0,4
	8	39,4	60	-	0,5

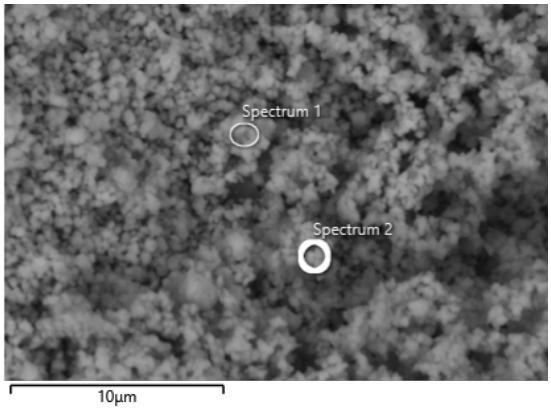

(a)

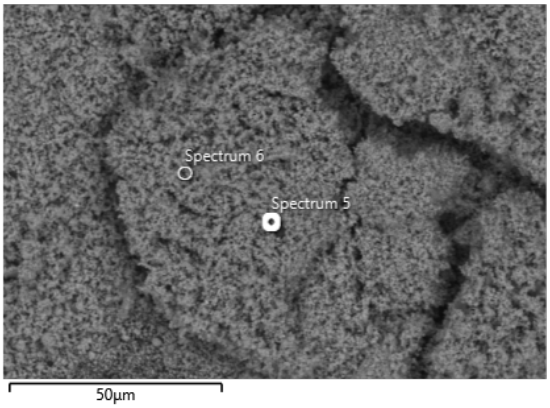

(b)

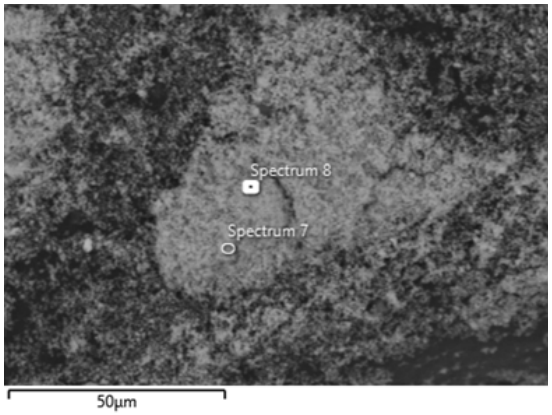

(c)

Fig. 4: EDS spectrum of (a) LTO/C 3% - 90 minutes (b) LTO/C 3% - 120 menit (c) LTO/C 3% - 150 menit

3.4 Conductivity of activated carbon and LTO/C

EIS characterization resulting the semi-circle Nyquist curve, the top of the curve is R_e (electrolyte resistance) and the the curve intercept with x-axis is R_{ct} (charge transfer resistance). R_e is the resistance of electrolyte component, separator and the electrode[17]. Figure 5a shows that the activated carbon resistance is high which mean that it is still less conductive and confirmed by the low conductivity as calculated in table 2. Figure 5b depicted the samples R_e from the lowest respectively, of LTO/C 3% - 90 minutes, LTO/C 3% - 120 minutes, LTO/C 3% - 150 minutes. The R_e can be increasing by the existence of passive layer growth on the electrode surface due to deposition of electrolyte and the instability of electrolyte during the testing[18]. Other probability is because there was the structural change due to particle microcrack[19].

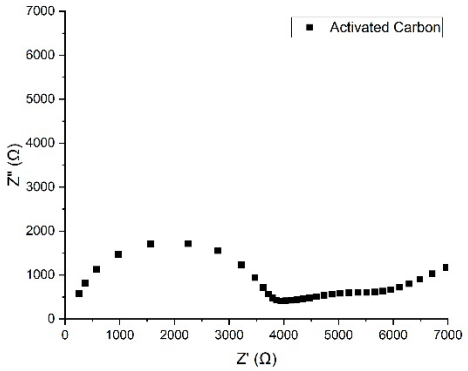

(a)

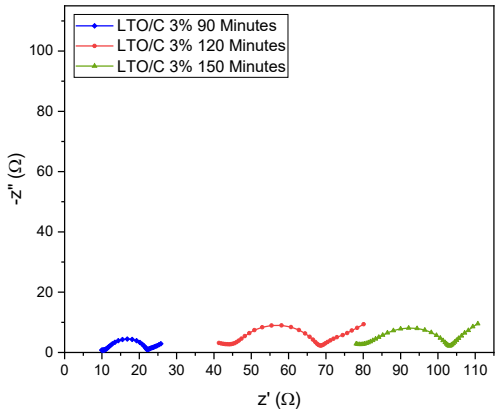

(b)

Fig. 5: EIS results of (a) activated carbon (b) LTO/C composites

The conductivity was calculated from the EIS result using equation 1. R_b is the bulk resistance or equal to R_{ct}, l is the coating thickness, and A is the surface area of coin. The carbon active resulting the conductivity of $9{,}65.10^{-5}$ S/m and successfully increased the conductivity of the three LTO/C samples. LTO/C 3% - 90 minutes has highest conductivity between the three samples. The ball-milling process resulting the less agglomerated and smaller size particles which increase the conductivity[20]. The increase of conductivity was also affected by the addition of activated carbon addition as the conductive particle[21]. LTO/C 3% - 120 minutes has lowest conductivity compared to the other two samples, this confirmed by the more agglomerated particle on the previous characterization

$$\sigma = \frac{l}{R_b A} \qquad (1)$$

Table 3. Conductivity of activated carbon and LTO/C composites

Sample	*l* (m)	Rct (Ω)	A (m^2)	Conductivity (S/m)
Activated Carbon	0,0075	3867,2	0,0064	$9,65.10^{-5}$
LTO/C 3% - 90 Minutes		12,2413		$3,05.10^{-2}$
LTO/C 3% - 120 Minutes		27,2946		$1,37.10^{-2}$
LTO/C 3% - 150 Minutes		24,9722		$1,49.10^{-2}$

3.5 Cyclic Voltammetry of LTO/C

The cyclic voltammetry testing resulting the cathodic and anodic curve where each peak identified the potential value. Figure 6 depicted the peaks of all sample are relatively symmetric, this shows that the samples have good reversibility. The cyclic voltammetry testing also inform the specific capacitance from the samples. The three samples have anodic and cathodic peak near 1,55 V which is the LTO theoretically potential value.

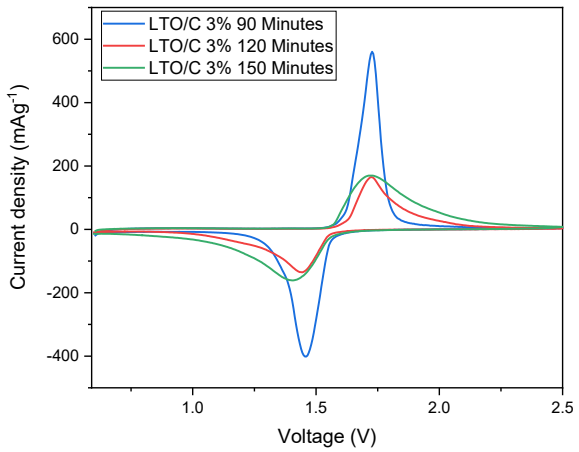

(a)

Fig. 6: Cyclic Voltammetry testing of LTO/C composites

The table 3 shows the polarization, specific capacity and working potential (E^0). The highest specific capacitance was achieved by LTO/C 3% 90 minutes followed by LTO/C 3% 150 minutes and LTO/C 3% 120 minutes. The conductivity is consistence with the EIS characterization. LTO/C 3% 90 minutes has highest and sharpest peak that indicate the fast charge-discharge process. LTO/C 3% 120 minutes, again, shows the poorest result as occurred in EIS characterization. This might because the agglomeration in the LTO/C 3% 120 minutes slurry on the mixing process. Agglomeration resulting in capacity lost due to reduction of surface area[22, 23].

Table 4. Conductivity of activated carbon and LTO/C composites

Sample	E^0 (V)	Polarization	Specific Capacity (mAh/g)
LTO/C 3%-90 Minutes	1,5935	0,267	149,8
LTO/C 3%-120 Minutes	1,5845	0,281	110,71
LTO/C 3%-150 Minutes	1,5600	0.316	137,63

3.6 Charge-Discharge Testing of LTO/C

The charge-discharge testing informed the battery performance by the increasing of the cycles. The testing is conducted in 5 current rates which are C/2, 1C, 2C, 5C, 10C and 15C. Current rate is the current given on the certain time to the battery that will result the discharge capacity and changes in different cycles[24]. The optimum capacity of battery will be differed in each cycle where in C/2 the charge-discharge duration is 2 hours, in 1C the charge-discharge duration is 1 hours and the shortest duration in 15C is 4 minutes[25]. In figure 7a plateau can be seen in C/2 which similar as the characteristic of LTO. Meanwhile in the 15C, plateau was not formed because of the short duration. In the figure 7b, the LTO/C 3% 90 minutes reached specific capacity of 130 mAH/g on C/2 and 54 mAH/g on 15C which was the highest capacity compared to the two samples.

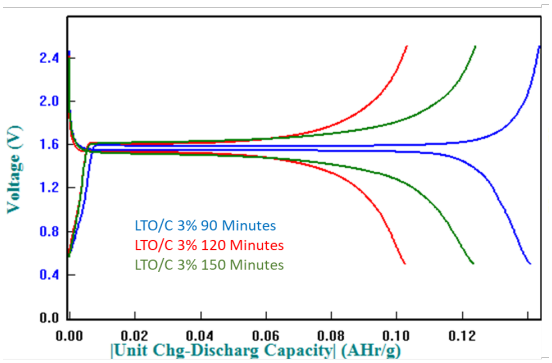

(a)

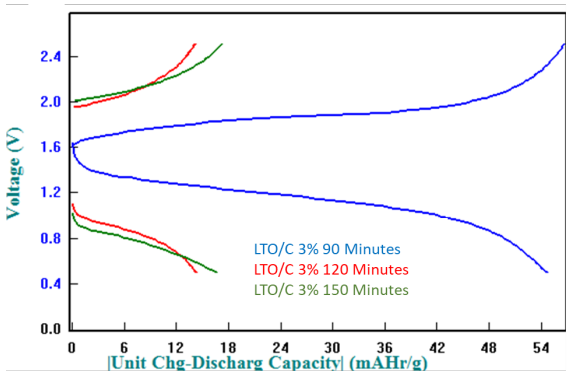

(b)

Fig. 7: Charge-discharge testing on (a) C/2 (b) 15C

The figure 8 shows the discharge capacity lost. In C/2 to 15C, the three sample have the consistence decrease where the highest to lowest capacity in all current rates respectively are LTO/C 3% 90 minutes, LTO/C 3% 150 minutes and LTO/C 3% 120. The LTO/C 3% 90 minutes shows best performance even in the high current rates.

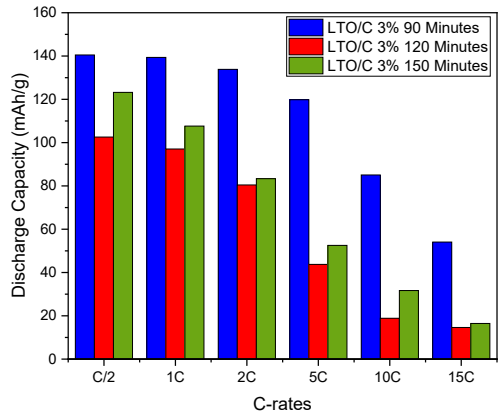

(a)

Fig. 8: Capacity lost of LTO/C composite from C/2 to 15C

4 Conclusion

The mixing time of activation of carbon and LTO can effecting the conductivity of the battery anode. In this research, LTO/C 3% which mixed for 90 minutes achieved highest conductivity of $3{,}05.10^{-2}$ S/m and resulting the highest capacity of 149,8 mAh/g. The agglomeration can decrease the mixture conductivity due to the high resistance which occured in LTO/C 3% 120 minutes, resulting the lowest specific capacity compared to the other mixtures.

Acknowledgements

The authors would like to express their gratitude for financial support from the Ministry of Education and Culture, Republic of Indonesia under PRN-BOPTN Project, with contract No : 008/E4.1/AK.04.PRN/2021.

References

1) R. Geyer, J. R. Jambeck, and K. L. Law, “Production, use, and fate of all plastics ever made,” *Sci. Adv.*, (2017) doi: 10.1126/sciadv.1700782.
2) Y. A. Hidayat, S. Kiranamahsa, and M. A. Zamal, “A study of plastic waste management effectiveness in Indonesia industries,” *AIMS Energy*, (2019) doi: 10.3934/ENERGY.2019.3.350.
3) J. R. Jambeck *et al.*, “Plastic waste inputs from land into the ocean,” *Science (80-.).*, (2015), doi: 10.1126/science.1260352.
4) S. Mao, X. Huang, J. Chang, S. Cui, G. Zhou, and J. Chen, “One-step, continuous synthesis of a spherical Li4Ti5O12/graphene composite as an ultra-long cycle life lithium-ion battery anode,” *NPG Asia Mater.*, **11** (7), 224–224, (2015). doi: 10.1038/am.2015.120.
5) X. Cai, L. Lai, Z. Shen, and J. Lin, “Graphene and graphene-based composites as Li-ion battery electrode materials and their application in full cells,” *J. Mater. Chem. A*, (2017), doi: 10.1039/c7ta04354f.
6) T. W. Hertzke, N. Müller, P. Schaufuss, S. Schenk, “Expanding electric - vehicle adoption despite early growing pains,” *McKinsey Co.*, (2019).
7) X. Guo *et al.*, “Solid-state synthesis and electrochemical performance of Li4Ti5O12/graphene composite for lithium-ion batteries,” *Electrochim. Acta*, **109**, 33–38, (2013), doi: https://doi.org/10.1016/j.electacta.2013.07.058.
8) Z. Xie, X. Li, W. Li, M. Chen, and M. Qu, “Graphene oxide/lithium titanate composite with binder-free as high capacity anode material for lithium-ion batteries,” *J. Power Sour.*, **273**,. 754–760, (2015), doi: https://doi.org/10.1016/j.jpowsour.2014.09.154.
9) K. Yu, J. Li, H. Qi, & C. Liang. (2018). High-capacity activated carbon anode material for lithium-ion batteries prepared from rice husk by a facile method. *Diam. Relat. Mater.*, **86**, 139-145.

doi:10.1016/j.diamond.2018.04.019
10) A. L. Cazetta, A. M. Vargas, E. M. Nogami,... & Almeida, V. C. NaOH-activated carbon of high surface area produced from coconut shell: Kinetics and equilibrium studies from the methylene blue adsorption. *Chem. Eng. J.*, ***174***(1), 117-125. doi: 10.1016/j.cej.2011.08.058
11) K. Thu, T. Miyazaki, K. Nakabayashi, J. Miyawaki, & F. Rahmawati.. Highly Microporous Activated Carbon from Acorn Nutshells and its Performance in Water Vapor Adsorption. *Evergreen*, **8** (1) 249-254. (2021) doi: 10.5109/4372
12) E. Raymundo-Pinero, P. Azaïs, T. Cacciaguerra, D. Cazorla-Amorós, A. Linares-Solano & F. Béguin, KOH and NaOH activation mechanisms of multiwalled carbon nanotubes with different structural organisation. *Carbon*, **43** (4), 786-795. doi: 10.1016/j.carbon.2004.11.005
13) L. Joncourt, M. Mermoux, P. H. Touzain, L. Bonnetain, D. Dumas & B. Allard. Sodium reactivity with carbons. *J. Phys. Chem. Sol.*, **57** (6-8), 877-882. (1996) doi: 0.1016/0022-3697(95)00366-5
14) Y. T. Li, Y. T. Pi, , L. M. Lu, S. H. Xu, & T. Z. Ren. Hierarchical porous active carbon from fallen leaves by synergy of K2CO3 and their supercapacitor performance. *J. Power Sour.*, **299**, 519-528. (2015) doi: 0.1016/j.jpowsour.2015.09.039
15) K. Babeł & K. Jurewicz. KOH activated lignin based nanostructured carbon exhibiting high hydrogen electrosorption. *Carbon*, **46** (14), 1948-1956. (2008) doi: 10.1016/j.carbon.2008.08.005
16) Nurohmah, A. R., Yudha, C. S., Rahmawati, M., Nisa, S. S., Jumari, A., Widiyandari, H., & Purwanto, A. (2021). Structural and Electrochemical Analysis of Iron Doping in LiNi_0. 6-x Mn_0. 2 Co_0. 2 Fe_x O_2 battery. **8** (1). 82-88. (2021) doi: 10.5109/4372263
17) B. Priyono, M. F. Fitratama, S. Roulli, A. Subhan, and A. Z. Syahrial, "Characterization of lto/silicon oxycarbide with activated carbon addition for anode of lithium-ion batteries," in *1000 MSF,* Materials Science Forum, 3–11 (2020).
18) X. Cai, L. Lai, Z. Shen, & J. Lin. Graphene and graphene-based composites as Li-ion battery electrode materials and their application in full cells. *J. Mater. Chem. A*, **5** (30), 15423-15446. (2017) doi: 10.1039/C7TA04354F
19) W. Choi, H. C. Shin, J. M. Kim, J. Y. Choi, & W. S. Yoon. Modeling and applications of electrochemical impedance spectroscopy (EIS) for lithium-ion batteries. *J. Electrochem. Sci. Tech.*, **11** (1), 1-13. (2020) doi: 10.33961/jecst.2019.00528
20) K. Hashizaki, S. Dobashi, S. Okada, T. Hirai, & Z. Ogumi. Charge-Discharge Characteristics of Li/CuCl_2 Batteries with LiPF_6/Methyl Difluoroacetate Electrolyte. *Evergreen*, *6*(1), 1-8. (2019) doi: 10.5109/2936213
21) K. Hashizaki, S. Dobashi, S. Okada, T. Hirai, J. I. Yamaki, & Z. Ogumi. Charge-Discharge Characteristics of Li/CuCl_2 Batteries with LiPF_6/Methyl Difluoroacetate Electrolyte. *Evergreen*, *6*(1), 1-8. (2019) doi: 10.5109/2320995
22) Annisa, N., Orlando, I., & Syahrial, A. Z. (2019, November). Effect of Activated Carbon Addition on Electrochemical Performance of Li4Ti5O12/Nano Si Composite as Anode Material for LiB. In *IOP Conference Series: Materials Science and Engineering*, **553** (1). IOP Publishing.
23) Zulfia A., Margaretha Y. R., Priyono B., and Subhan A. Synthesis of LTO nanorods with Ac/nano-Si composite as anode material for Lithium-ion batteries. *Int. J. Technol.*, **9** (6), 1225–1235. (2018). doi: 10.14716/ijtech.v9i6.2444.
24) Tsubota, T., Kitajou, A., & Okada, S. O3-type na (Fe_1/3Mn_1/3CO_1/3) O_2 as a cathode material with high rate and good charge-discharge cycle performance for sodium-ion batteries. *Evergreen*, **6** (4), 275-279. (2019) doi: 10.5109/2547348
25) Nakamoto, K., Sakamoto, R., Kitajou, A., Ito, M., & Okada, S. Cathode properties of sodium manganese hexacyanoferrate in aqueous electrolyte. *Evergreen*. **6** (4), 275-279, (2017). doi: 10.5109/2547348